Effect of grain refinement on deformation behavior of technical grade titanium under tension

A. V. Eremin, S. V. Panin, A. V. Byakov, Yu. P. Sharkeev, A. Yu. Eroshenko, and A. M. Mairambekova

Citation: AIP Conference Proceedings **2051**, 020076 (2018); doi: 10.1063/1.5083319
View online: https://doi.org/10.1063/1.5083319
View Table of Contents: http://aip.scitation.org/toc/apc/2051/1
Published by the American Institute of Physics

Effect of Grain Refinement on Deformation Behavior of Technical Grade Titanium under Tension

A. V. Eremin[1,a)], S. V. Panin[1,2], A. V. Byakov[1], Yu. P. Sharkeev[1,2], A. Yu. Eroshenko[1], and A. M. Mairambekova[1,3]

[1] *Institute of Strength Physics and Materials Science, Tomsk, 634055 Russia*
[2] *National Research Tomsk Polytechnic University, Tomsk, 634050 Russia*
[3] *National Research Tomsk State University, Tomsk, 634050 Russia*

[a)] Corresponding author: ave@ispms.ru

Abstract. The paper deals with the study on the impact of grain refinement by severe plastic deformation upon the microstructure, as well as deformation and fracture behavior under tensile loading of technical grade titanium. The microstructure of coarse- and ultra-fine grain technical grade titanium was investigated by optical, transmission electron microscopy and X-ray diffraction. In situ monitoring of deformation behavior was conducted by means of acoustic emission and digital image correlation. Scanning electron microscopy was employed for fracture surface observation. The results of the tensile tests have revealed significant growth in ultimate strength and decrease of ductility due to grain-boundary strengthening. The experimental data obtained allow one to get the appropriate understanding of the mechanisms responsible for variation of mechanical properties and fracture patterns as well as to attain quantitative estimation of strain localization induced by the grain refinement.

INTRODUCTION

According to the US Industry Study [1] due to high biocompatibility titanium and its alloys have wide prospects in medical applications for manufacturing implants and prostheses. It is known that implants during life time are subjected to high cyclic loads. However, low mechanical properties of technical grade titanium (first of all, yield limit and ultimate strength) prevent its application for fabrication heavily loaded components (for instance, prostheses of musculoskeletal system or dental implants. Addition of doping elements gives rise to increasing mechanical properties, but results in (i) reduction of biocompatibility, (ii) release of toxic elements into the human body [2], and (iii) increase of manufacturing costs. An alternative approaches consists in developing alloys containing only nontoxic doping elements [3] when enhanced mechanical properties are attained through the nanostructuring via severe plastic deformation (SPD) [4, 5].

The purpose of the study is to investigate the grain refinement effect upon microstructure, mechanical properties and both deformation behavior and fracture kinetics of technical grade coarse-grain (CG) and ultrafine-grain (UFG) grain titanium grade 2 under quasi-static tensile loading by means of combined acoustic-optical monitoring (by acoustic emission and digital image correlation) and fracture surface SEM observation.

EXPERIMENTAL PROCEDURE

Mechanical properties were determined under quasi-static tension with the help of electromechanical testing machine Instron 5582. The cross-head speed was equal to 0.2 mm/min. Two types of the samples were employed: in the initial CG state and after severe plastic deformation (UFG). The miniature specimens for the tensile tests had the gauge length of 14 mm and cross-section of 1×3 mm. In situ data on the deformation process was obtained by means of digital image correlation technique (DIC)—optical and noncontact method for acquisition strain fields on

Proceedings of the Advanced Materials with Hierarchical Structure for New Technologies and Reliable Structures
AIP Conf. Proc. 2051, 020076-1–020076-5; https://doi.org/10.1063/1.5083319
Published by AIP Publishing. 978-0-7354-1777-9/$30.00

the specimen surface. Optical images have the resolution of 2454×2056 pixels with observation area of 11.3×9.5 mm (scale 4.6 μm/pixel). Images were processed with the help of Vic-2D software (Correlated solutions, USA).

DIC observation under loading was combined with registration of acoustic emission (AE). The following equipment was employed: analog-to-digital board LA-n150-14PCI with 14 bit resolution and sampling frequency of 3 MHz (Rudnev–Shilyaev, Russia), acoustic emission transducer WD (Physical Acoustics Corporation, USA), and analog signal amplifier (ISPMS SB RAS, Russia) with the gain of 40 dB.

In situ registration of optical images and acoustic emission signals allows one to analyze the kinetics of deformation and fracture processes with attaining numerical estimates of their evolution in time/strain domain.

REFINEMENT PROCEDURE AND MICROSTRUCTURE STUDY

The UFG structure in technical grade titanium (grade 2) was formed in two-stage combined severe plastic deformation (SPD) procedure, which includes abc-pressing with a multipass rolling in grooved rollers [6, 7]. At the first stage the deformation of the billets was carried out in a hydraulic press at the strain rate of 10^{-3}–10^{-1} s^{-1}. After each pressing step the billet was rotated by 90° and then it underwent the next cycle (the total number of pressing cycles was three). The temperature of the billet was decreased gradually in the range from 500 to 400°C. Relative strain value of the billet in each pressing cycle did not exceed 40–45%.

At the second stage the billets were processed (deformed) by rolling in grooved rollers at room temperature. The total strain during the rolling was 90%. In order to reduce internal stresses the final blanks with dimensions of $\sim 1.5 \times 8 \times 25$ mm (thickness×width×length) were annealed at $T = 350$°C for $t = 1$ hour.

The microstructure of the samples was investigated by optical microscopy (Carl Zeiss Axio Observer) and transmission electronic microscopy (JEOL JEM 2100). The average size of structural elements (grains, subgrains, fragments) was calculated using intercept length method [8].

It is shown that the CG titanium (Fig. 1a) has α-phase grains (average grain size of 25 μm). The UFG titanium microstructure is presented in Fig. 1b. Bright-field TEM image shows subgrains and fragments with the equiaxial shapes. However their structural state is nonequilibrium. The boundaries between grains are poorly visible ("blurred"). Also, substructures with high dislocation density are evident. The subgrain boundaries are barely discernible and could be found inside the grains. Extinction contours evidence for high residual stress level in the material after the SPD. The average size of structural elements, including grains, subgrains, fragments is equal to ≈0.2 μm.

Reflexes at the microdiffraction pattern (the inset in Fig. 1b) are circle arranged, indicating presence of high-angle boundaries, while azimuth diffusion testifies for high level of internal stresses. No reflections attributed to titanium α-phase are evident at the microdiffraction pattern; thus one can conclude that the UFG titanium consists of β-phase only.

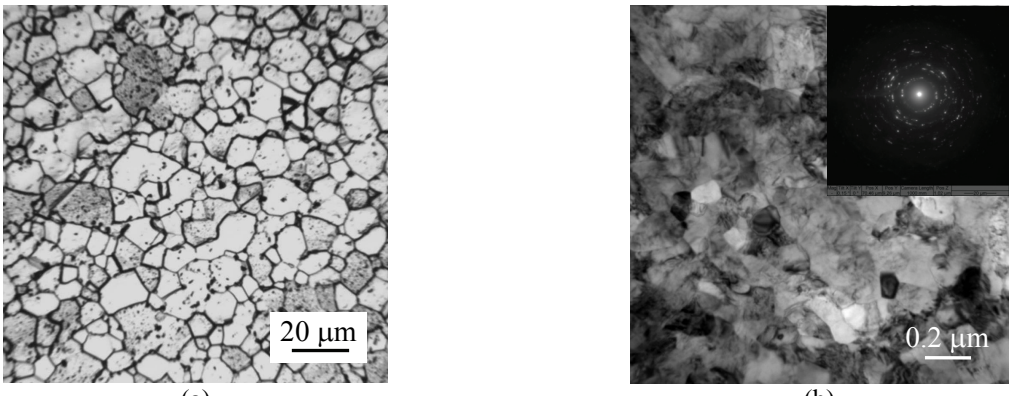

(a) (b)

FIGURE 1. Optical image of coarse-grained titanium (a) and bright-field TEM image of ultrafine-grained titanium (b). The inset in (b) illustrates the microdiffraction pattern

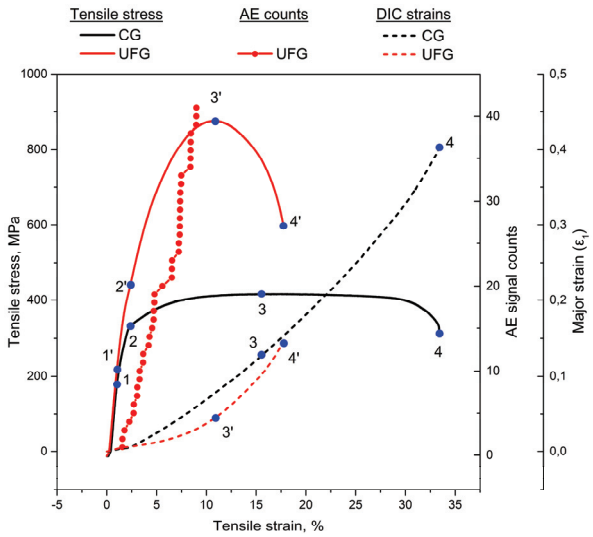

FIGURE 2. Stress-strain curves for CG and UFG titanium (solid line), counts of AE signals for UFG Ti (circles) and major strains, obtained by the DIC method (dash line). Blue points with numbers (apostrophe for UFG specimens) depict critical points of the curves

RESULTS AND DISCUSSION

Figure 2 demonstrates the stress-strain curves for the two type specimens with the plot on the corresponding AE signal counts and averaged major strains ε_1 measured by DIC. The measured mechanical properties of CG and UFG titanium are presented in Table 1.

It is seen from stress-strain diagrams as well as data on mechanical properties (Table 1) that the UFG titanium possesses much higher ultimate tensile strength (UTS) and yield stress. The Young moduli are equal for both types of materials. Since grain refinement gives rise to increasing the fraction of grain boundaries. The latter act as obstacles for dislocation gliding and require higher external load (energy) to overpass them. This phenomenon is responsible for increasing the yield strength (that agrees well with Hall–Petch law). Further loading results in much more pronounced differences in deformation behavior between the CG and UFG materials.

The AE registration threshold was set equal for both types of materials. This enables us to reveal that the initial state CG titanium under stress does not emit any signals of significantly high-amplitude. However, loading of the UFG Ti results in extensive generation of acoustic waves which are more likely attributed to dislocation bunch formation. We also suggest that subsequent release of the accumulated energy comes from the microfracture processes. Note, that first AE signals were registered just after the onset of plastic deformation (point 2′).

In situ DIC monitoring provides qualitative (visual patterns in terms of strain fields) and quantitative (strain values at each local region point on the specimen surface) data on the deformation behavior. Figure 3 illustrates the strain fields for the CG (images a–d) and the UFG titanium (images e–h) at the moments corresponding to the points marked at the stress-strain curves in Fig. 2. It is seen that at $\varepsilon = 1\%$ (Figs. 3a, 3e) the deformation possesses elastic and uniform pattern: the mean values of major strains ε_1 (presented in Fig. 2 by dashed lines) are nearly the same. With increasing the strain ($\varepsilon = 2.3\%$, Figs. 3b, 3f) the deformation field for the UFG specimen remains almost constant while the CG ones exhibit certain strain localization in the central part with twofold increase of maximum strain (from 0.004 to 0.009).

TABLE 1. Mechanical properties of CG and UFG titanium

Material	Ultimate tensile strength, MPa	Stain at break, %	Yield stress, MPa	Yield strain, %
CG titanium	419 ± 6	32 ± 2.7	198 ± 17	1.10 ± 0.08
UFG titanium	863 ± 6	15 ± 2.3	244 ± 23	1.11 ± 0.12

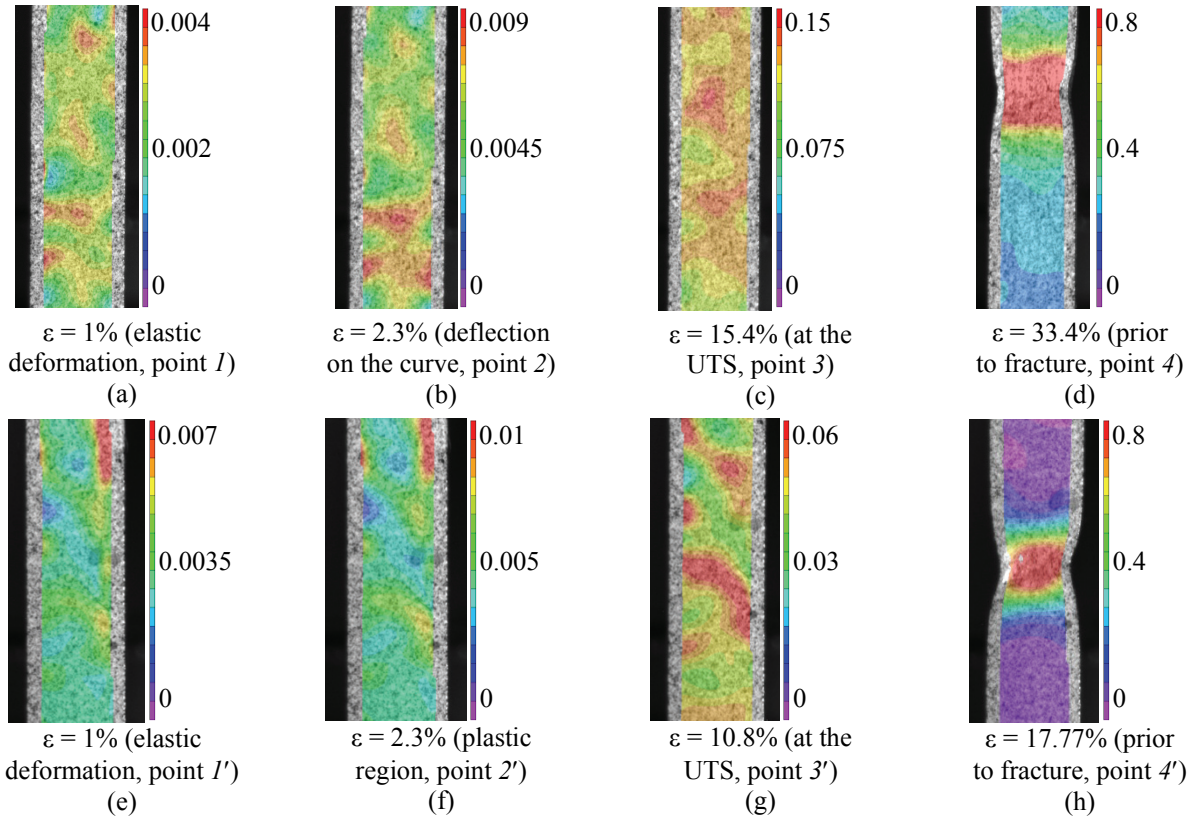

FIGURE 3. Patterns of the major strain fields (ε_1) measured by the DIC technique. Each image corresponds to the points depicted in Fig. 2 on stress–strain curves. Images (a–d)—CG titanium; (e–h)—UFG titanium

Further loading of the CG titanium results in plastic flow initiation, which is manifested through the nonlinear behavior of stress-strain curve and parabolic growth of ε_1 (Fig. 2, DIC strain patterns for the CG Ti). Strain field in Fig. 3c shows the deformation spreading over the larger area with involvement larger materials' portions in the plastic flow. Thus the plastic deformation is uniformly distributed over the specimen gauge length. Further, the strain tends to localize while neck is progressively formed for a long time; in doing so most of the deformation processes occur in the neck area.

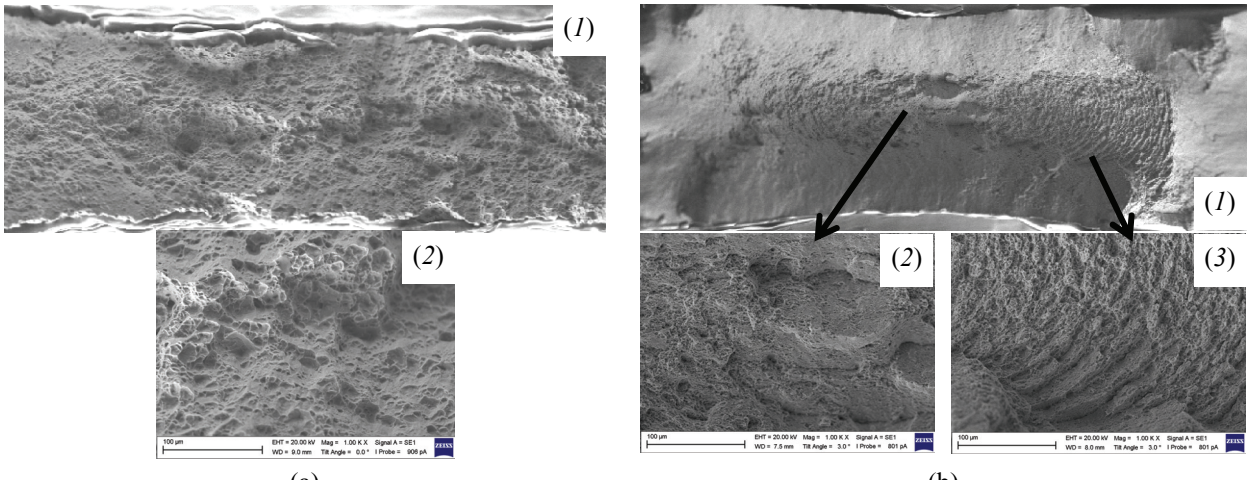

FIGURE 4. SEM micrographs of fracture surface for: (a) CG titanium—panoramic view (*1*), image taken at high magnification (*2*); (b) UFG titanium—panoramic view (*1*), central part of the fracture surface (*2*), ductile step-like fracture pattern (*3*)

We suggest the higher area of grain boundaries in the UFG titanium suppresses earlier plastic deformation development, while it demonstrates higher rate of the strain growth (Fig. 2, point *2′*) as well as the necking process (Fig. 2, point *3′*) as compared with the CG Ti. At the same time the plastic flow localization also takes place, however in contrast with the CG titanium it was not developed over a small region, i.e. it was arrested by grain boundaries in the specimen's central part (Fig. 3g).

Figures 3d and 3f demonstrate the specimens strain fields at the moment prior to fracture. One can reveal the difference in the fracture process development: the CG Ti exhibits the normal tearing due to high ductility and easy dislocation gliding, while the UFG one is fractured mainly by the shear stresses being oriented at the angle of 45° to the loading axis.

SEM micrographs of fracture surface for the CG and UFG titanium are presented in Figs. 4 and 5 correspondently. The texture of the fracture surface for the CG Ti is uniform and represents the normal tearing with significant ductility. Fracture surface pattern for the UFG Ti consists of three different zones: (i) central region (fracture onset), (ii) two regions with step-like ductile fracture textures on the right and left side from the central part that develop through the specimen cross section, and (iii) the region with smooth surfaces on the specimen periphery resulted from the action of shear stresses (oriented at the angle of 45° to the loading axis). Three types of fracture textures are attributed to the variation in deformation mode. The middle region was formed due to normal tearing under the plane strain conditions (in presence of constraints caused by surrounding material). The smooth surface regions on the periphery were under plane stress state and exhibit shear fracture pattern. The regions with the step-like ductile texture are transient zones between various fracture modes.

CONCLUSION

The significant difference in the deformation and fracture mechanisms of the CG and UFG technical grade titanium has been revealed. It is shown that the grain size refinement results in the twofold increase of the UTS (from 419 to 863 MPa) and double reduction of elongation at break (from 32 to 15%). However the yield stress and yield strain do not changed much. The CG titanium does not emit high level AE signals while under loading of the UFG Ti such signals are registered being attributed to energy release from the dislocation bunches. Larger area of grain boundaries in the UFG Ti suppresses uniform plastic flow there with involving less material into developed plastic flow. The latter becomes evident from the DIC studies. SEM fractography analysis has shown the difference in fracture surface patterns: the CG Ti exhibits uniform ductile fracture resulted from the normal tearing, whereas the UFG Ti fracture surface contains three various zones attributed to different failure processes (normal tearing, transient zone and shear fracture).

ACKNOWLEDGMENTS

The work was supported by President Scholarship for young scientists and graduate students in 2018-2020 (reference number SP-198.2018.4). SEM fractography was performed by LEO EVO 50 microscope in "NANOTECH" of ISPMS SB RAS.

REFERENCES

1. "Biocompatible materials", in *US Industry Study with Forecasts to 2010 & 2015* (The Freedonia Group, USA, 2006), p. 264.
2. M. Browne and P. J. Gregson, Biomaterials **21**, 385–392 (2000).
3. M. Niinomi, Metal. Mater. Trans. A **33**, 477–486 (2002).
4. I. A. Ovid'ko and T. G. Langdon, Rev. Adv. Mater. Sci. **30**, 103–111 (2012).
5. R. Z. Valiev, I. Sabirov, A. P. Zhilyaev, and T. G. Langdon, JOM **64**, 1134–1142 (2012).
6. Yu. P. Sharkeev, A. Yu. Eroshenko, V. I. Danilov, et al., Russ. Phys. J. **56**, 1156–1162 (2014).
7. Yu. P. Sharkeev, A. Yu. Eroshenko, I. A. Glukhov, et al., in *Physical Mesomechanics of Multilevel Systems 2014, AIP Conf. Proc.*, vol. **1623**, edited by V. E. Panin, S. G. Psakhie, V. M. Fomin (American Institute of Physics, Melville, NY, 2014), pp. 567–570.
8. ASTM E1382-97 (2015).